Design of Highly Stable, Ordered Cage Mesostructured Monoliths with Controllable Pore Geometries and Sizes

Sherif A. El-Safty,* Takaaki Hanaoka, and Fujio Mizukami

Laboratory for Membrane Chemistry, Tohoku Center, National Institute of Advanced Industrial Science and Technology (AIST), 4-2-1 Nigatake, Miyagino-ku, Sendai, 983-8551, Japan

Received January 4, 2005. Revised Manuscript Received April 19, 2005

A simple strategy in terms of fabrication time (within minutes) and composition phase domains was used to design optical cage mesostructured silica monoliths with shape- and size-controlled cavities and entrance pores, large-sized glass (crack-free), thick-walled framework up to 20 nm thick, uniformly sized mesopores of ∼14 nm, and cubically ordered geometries. This is the first report of using a rapid templating method in microemulsion systems to fabricate mesoscopically ordered silica/copolymers composites that have cage structures. With use of this strategy, which is based on an instant direct-templating method, the size of the cavities and entrance pores of highly ordered monolithic cages (designated as HOM-C) were enlarged by a high concentration of copolymers ($EO_mPO_nEO_m$) used in the composition phase domains, by a high degree of swelling, and by large PO−EO blocks (core−corona) of the copolymer templates. Our strategy enables actual control over the phase structures of the copolymers. Thus, a family of cubic cage mesostructured monoliths was feasibly fabricated in large orientationally ordered domains. The HOM-C structures fabricated here exhibited long-term retention (about a month) of the hierarchically ordered structures under extreme hydrothermal conditions. Our results show evidence that the size and shape of the connecting pores and the nature of the spherical cavity of the cage geometry crucially influenced the retention of the HOM-C cage character when the monolith was subjected to hydrothermal treatment such as boiling water.

Introduction

Ordered nanostructured molecular sieves with controllable pore geometry and nanoscale size (2−30 nm) are of technological interest due to potential widespread applications.[1] Organic molecule-templated synthesis strategies are commonly used to direct the design of materials that have a variety of ordered architectures in 2D and 3D (two- and three-dimensional, respectively).[2−8] Among all possible surfactant templates, the amphiphilic triblock copolymers of Pluronic-types ($EO_mPO_nEO_m$) have been described as the most commonly used systems to develop mesoporous materials that are highly ordered and have large pore dimensions (up to 10 nm) without the use of swelling agents and to develop thicker wall structures that have improved hydrothermal stability compared with that of the parent MS41 family.[3] The 3D cubic morphologies show particular promise for advanced functionalities, such as unique nanostructured designs composed of metals,[9] semiconductors,[10] composites,[11] and carbons.[12] Ordered cubic mesostructures with cage-like structures are desirable in terms of their potential, among all 3D mesostructured materials. Due to the well-defined pore sizes of spherical cavities and the connectivity among pores,[13] the 3D cage structures are promising in many practical applications, such as separation of protiens,[14] electronics,[15] catalytic surfaces and supports,[16] sensing,[17] and inclusion chemistry.[18]

Cage structures such as cubic *Pm*3*n* (SBA-1)[19] and 3D hexagonal $P6_3/mmc$ (SBA-2)[20] have been fabricated using alkylammonium surfactants under acidic and basic conditions, respectively, whereas cubic *Fm*3*m* with intergrowth

* To whom correspondence should be addressed. E-mail: sherif.el-safty@aist.go.jp.
† E-mail: f-mizukami@aist.go.jp.

(1) (a) Davis, M. E. *Nature* **2002**, *417*, 813. (b) Regan, B. C.; Aloni, S.; Ritchie, R. O.; Dahmen, U.; Zettl, A. *Nature* **2004**, *428*, 924. (c) Rustom, A.; Saffrich, R.; Markovic, I.; Walther, P.; Gerdes, H. *Science* **2004**, *303*, 1007.
(2) Kresge, C. T.; Leonowicz, M. E.; Roth, W. J.; Vartuli, J. C.; Beck, J. S. *Nature* **1992**, *359*, 710.
(3) Zhao, D.; Huo, Q.; Jianglin, F.; Chmelka, B. F.; Stucky, G. D. *J. Am. Chem. Soc.* **1998**, *120*, 6024.
(4) Liu, X.; Tian, B.; Yu, C.; Gao, F.; Xie, S.; Tu, B.; Che, R.; Peng, L.-M.; Zhao, D. *Angew. Chem. Int. Ed.* **2002**, *41*, 3876.
(5) Che, S.; Garcia-Bennett, A. E.; Yokoi, T.; Sakamoto, K.; Kunieda, H.; Terasaki, O.; Tatsumi, T. *Nat. Mater.* **2003**, *2*, 801.
(6) Bagshaw, S. A.; Prouzet, E.; Pinnavaia, T. J. *Science* **1995**, 269, 1242.
(7) Cha, J. N.; Stucky, G. D.; Morse, D. E.; Deming, T. J. *Nature* **2000**, *403*, 289.
(8) Che, S.; Liu, Z.; Ohsuna, T.; Sakamoto, K.; Terasaki, O.; Takashi, T. *Nature* **2004**, *429*, 281.
(9) Joo, S. H.; Choi, S. J.; Oh, I.; Kwak, J.; Liu, Z.; Terasaki, O.; Ryoo, R. *Nature* **2001**, *412*, 169.
(10) Trikalitis, P. N.; Rangan, K. K.; Bakas, T.; Kanatzidis, M. G. *Nature* **2001**, *410*, 671.
(11) Tian, B.; Liu, X.; Solovyov, L. A.; Liu, Z.; Yang, H.; Zhang, Z.; Xie, S.; Zhang, F.; Tu, B.; Yu, C.; Terasaki, O.; Zhao, D. *J. Am. Chem. Soc.* **2004**, *126*, 865.
(12) Choi, M.; Ryoo, R. *Nat. Mater.* **2003**, *2*, 473.
(13) Sakamoto, Y.; Kaneda, M.; Terasaki, O.; Zhao, D. Y.; Kim, J. M.; Stucky, G. D.; Shin, H. J.; Ryoo, R. *Nature* **2000**, *408*, 449.
(14) Fan, J.; Yu, C.; Lei, J.; Tian, B.; Wang, L.; Luo, Q.; Tu, B.; Zhou, W.; Zhao, D. *Angew. Chem., Int. Ed.* **2003**, *42*, 3146.
(15) Timoshevskii, V.; Connetable, D.; Blasé, X. *Appl. Phys. Lett.* **2002**, *80*, 1385.
(16) Murakami, Y.; Yamakita, S.; Okubo, T.; Maruyama, S. *Chem. Phys. Lett.* **2003**, *375*, 393.
(17) Wirnsberger, G.; Scott, B. J.; Stucky, G. D. *Chem. Commun.* **2001**, 119.
(18) Antochshuk, V.; Kruk, M.; Jaroniec, M. *J. Phys. Chem. B* **2003**, *107*, 11900.

10.1021/cm050013h CCC: $30.25 © 2005 American Chemical Society
Published on Web 05/20/2005

(SBA-12) has been fabricated using Brij 76 surfactant under acidic conditions.[3,21] However, the utility of these cage structures, particularly in inclusion chemistry, has been inhibited by the restrictive syntheses (under basic or even under acidic conditions), by the structural complexity of the intergrowth mesophases, and by the limited pore sizes up to 4.0 nm.[18] Recently, large pore cages (>7 nm in diameter) of cubic *Fm*3*m* (FDU-, KIT-types)[14,22] and *Im*3*m* (SBA-16) have been fabricated using copolymer templates under acidic conditions.[3,13] Although syntheses of these cage materials yielded ordered cage structures with large pore size up to 12 nm, the potential of these materials could be impeded by the intensive, time-consuming, and hydrothermal synthesis conditions required and by the powdery products in small domain sizes. If ordered 3D cage structures can be fabricated by simple, reproducible synthesis designs into optically translucent monoliths that are crack-free at the macroscopic length scale, then their applications can be widely expanded.[1,23]

A synthesis design that achieves reliable control over the microstructure phase of the templates and over the final mesostructured replicas can possibly be used to design large mesoscopically ordered domains with a variety of mesophases.[24] Flexibility in controlling the 3D geometrical cage shape and size is of interest in potential catalysts and sorbents because 3D morphology and cage functionality should allow efficient transport of guest species via much more direct and easier diffusion to the network sites.[13,14,16] Furthermore, the development strategy that leads to high retention of the mesostructured frameworks subjected to hydrothermal treatments remains a significant challenge in materials synthesis. Due to the amorphous character of network pores, the hierarchical structures might collapse under boiling or even under steaming. Recent effort to improve the synthesis methodologies has led to hydrothermally stable frameworks.[25,26] However, the complexity of the stabilization procedures that result in a relatively poor mesoscopic ordering in the mesopore architectures could limit the facile and potential commercial applications of these materials in the petrochemical industry.

Here we developed a design strategy that is simple and fast, yet reproducible, and fulfills the growing demand for production yield of nanostructured materials for preparing cage-like mesostructures. This strategy, based on instantly preformed liquid-crystalline phases, seems promising as a broadly applicable method for controlling the mesophase domains and morphologies of templates and controlling the extended long-range ordering in the final monolithic replicas. This is the first report of using a rapid templating method in microemulsion systems to synthesize highly ordered silica/copolymers composites that have cage structures. In this study, a family of highly ordered cubic cage silica monoliths (HOM-C) with *Ia*3*d*, *Pm*3*n*, *Im*3*m*, and *Fm*3*m* symmetries, large spherical cavities of 14 nm, and pore entrance sizes up to 9.8 nm was successfully prepared using microemulsion liquid-crystal phases of commercial copolymers as templates. These cage structures exhibited unprecedented hydrothermal stability in boiling water. Long-term retention of both the orientational ordering (1−3 days) and the hierarchical framework (for a month or even longer) was achieved.

Experimental Section

Chemicals. All materials were used as produced without further purification. Triblock poly(ethylene oxide)−poly(propylene oxide)−poly(ethylene oxide) [designated as $EO_mPO_nEO_m$] copolymers and tetramethyl orthosilicate (TMOS), which was used as the silica source, were obtained from Sigma-Aldrich Company Ltd., USA. The copolymer surfactants were Pluronic P123 ($EO_{20}PO_{70}EO_{20}$, M_{av} = 5800), Pluronic F68 ($EO_{80}PO_{27}EO_{80}$, M_{av} = 8400), and Pluronic F108 ($EO_{141}PO_{44}EO_{141}$, M_{av}= 14.600) copolymers, where EO is $-CH_2-CH_2O-$ (hydrophilic part, or corona) and PO is $-CH_2(CH_3)CH-O-$ (hydrophobic part, or core). The EO content was 30, 80, and 83 wt % for P123, F68, and F108 copolymers, respectively. The solublizing agents of hydrocarbon alkanes with different alkyl chains, such as octane and nonane (C_nH_{2n+2}) and 1,3,5-trimethylbenzene ($C_6H_3(CH_3)_3$, or TMB), were obtained from Wako Company Ltd., Osaka, Japan.

Synthesis of Cubic Cage Silica Monoliths. A family of highly ordered cubic cage silica monoliths (HOM-C) was synthesized by using triblock copolymers (P123, F68, and F108) in the instantly direct templating liquid-crystal phase, as recently reported.[24] For example, synthesis of cubic *Im*3*m* cage-like monoliths (HOMC-1) at a F108/TMOS mass ratio of 35 wt % in the lyotropic systems was as follows. First, 0.7 g of F108 and 2 g of TMOS were dissolved in a flask by shaking in a water bath at 50−60 °C for 1−2 min, thus yielding a clear solution (i.e., homogeneous). Then, 1 g of H_2O/HCl (pH = 1.3) was quickly added to this solution. The mass ratio of F108:TMOS:H_2O/HCl was 0.7:2:1. Synthesis of other monolithic samples at various copolymer/TMOS ratios was done using the same procedure. The amount of copolymer was varied at 1.0, 1.4, and 1.6 in the mixture composition to fabricate cage mesophases with copolymer/TMOS mass ratios of 50, 70, and 80 wt %, respectively (Table 1).

In the quaternary microemulsion system (copolymer:hydrocarbon:TMOS:H_2O), the hydrocarbons were dissolved in the copolymers prior to the addition of the TMOS in all HOM-C syntheses. The amount ratio of copolymers to aliphatic hydrocarbons (alkane) was kept at 2:0.5. For all the syntheses of HOM-C monoliths, however, this amount ratio was increased to 2:1 when TMB was used as a solublizing agent added to the microemulsion phase designs to optimize both the swelling and the interfacial surface curvature of the copolymer micelles (Table 1). The composition mixture domains

(19) Huo, Q.; Margolese, D.; Ciesla, U.; Feng, P.; Gier, T. E.; Sieger, P.; Leon, R.; Petroff, P. M.; Schüth, F.; Stucky, G. D. *Nature* **1994**, *368*, 317.
(20) Huo, Q.; Petroff P. M.; Stucky, G. D. *Science* **1995**, *268*, 1324.
(21) Sakamoto, Y.; Diaz, I.; Terasaki, O.; Zhao, D.; Pérez-Pariente, J.; Kim, J. M.; Stucky, G. D. *J. Phys. Chem. B* **2002**, *106*, 3118.
(22) (a) Matos, J. R.; Kruk, M.; Mercuri, L. P.; Jaroniec, M.; Zhao, L.; Kamiyama, T.; Terasaki, O.; Pinnavaia, T. J.; Liu, Y. *J. Am. Chem. Soc.* **2003**, *125*, 821. (b) Kruk, M.; Jaroniec, M. *Chem. Mater.* **2003**, *15*, 2942. (c) Kleitz, F.; Liu, D.; Anilkumar, G. M.; Park, I.; Solovyov, L. A.; Shmakov, A. N.; Ryoo, R. *J. Phys. Chem. B* **2003**, *107*, 14296.
(23) (a) Nguyen, T. Q.; Wu, J. J.; Doan, V.; Schwartz, B. J.; Tolbert S. H. *Science* **2000**, *288*, 652. (b) Yang, P. D.; Wirnsberger, G.; Huang, H. C.; Cordero, S. R.; McGehee, M. D.; Scott, B.; Deng, T.; Whitesides, G. M.; Chmelka, B. F.; Buratto, S. K.; Stucky, G. D. *Science* **2000**, *287*, 465.
(24) (a) El-Safty, S. A.; Hanaoka, T. *Chem. Mater.* **2004**, *16*, 384. (b) El-Safty, S. A.; Hanaoka, T. *Adv. Mater.* **2003**, *15*, 1893. (c) El-Safty, S. A.; Mizukami, F.; Hanaoka, T. *J. Phys. Chem. B* **2005**, in press (on-line DOI: 10.1021/jp050304d).
(25) Liu, Y.; Pinnavaia, T. J. *J. Mater. Chem.* **2002**, *12*, 3179.
(26) On, D. T.; Kaliaguine, S. *J. Am. Chem. Soc.* **2003**, *125*, 618. (b) Kruk, M.; Celer, E. B.; Jaroniec, M. *Chem. Mater.* **2004**, *16*, 698. (c) Newalkar, B. N.; Komarneni, S.; Turaga, U. T.; Katsuki, H. *J. Mater. Chem.* **2003**, *13*, 1710.

Table 1. Structural Parameters of Cubic Cage-like Silica Monoliths (HOM-C) Synthesized in Microemulsion Systems of Copolymers; Mesopore (V_p)/Micropore (V_m) Volumes, Unit Lattice Dimension (a), BET Surface Area (S_{BET}), Cavity Pore Size (R), and Wall Thickness (W)

mesophase synthesis conditions											
copolymer templates	S/P[c] %	H[d]	T °C	cubic structure	V_P cm^3/g	V_m cm^3/g	a nm	S_{BET} m^2/g	R_{BJH} nm	(E-R)[a] nm	W[b] nm
P123	35	*e*	45	*Im*3*m*	0.55	0.07	12.5	523	5.4	(<4)	7.1
($EO_{20}PO_{70}EO_{20}$)	35	C_9	45		0.66	0.10	13.9	687	6.8	(<4)	7.1
	35	TMB^{0f}	45		0.58	0.09	12.5	510	6.0	(<4)	6.4
	35	TMB^2	45		0.66	0.11	15.0	550	7.2	(<4), (~6)	7.8
PF68	50		45	*Ia*3*d*	0.92	0.05	18.8	790	5.4	(<4)	13.4
($EO_{80}PO_{27}EO_{80}$)	50	TMB^0	45		1.10	0.07	19.7	961	5.6	(<4)	14.1
	70	C_8	45		1.28	0.08	21.7	920	6.4	(<4)	15.3
	70	C_9	45		0.92	0.08	24.0	645	7.2	(<4), (~6)	16.8
	50	TMB^1	45	*Pm*3*n*	1.00	0.08	19.7	860	6.4	(<4)	13.3
	50	TMB^2	45		0.88	0.08	22.4	721	6.8	(<4)	15.6
F108	35		45	*Im*3*m*	0.73	0.13	15.6	700	5.0	(<4)	10.6
($EO_{141}PO_{44}EO_{141}$)	35	C_9	45		0.50	0.13	15.6	604	6.0	(<4)	9.6
	35	TMB^0	45		0.50	0.13	15.6	742	6.4	(<4)	9.2
	70	TMB^0	50		1.01	0.11	20.8	755	12.2	(<4), (~8.4)	8.6
	80	–	50		1.90	0.09	17.8	1085	10.0	(<4), (~6)	7.8
	80	TMB^0	50		1.25	0.1	19.2	755	12.2	(<4), (~7.1, 9.1)	7.0
	35	TMB^2	45	*Fm*3*m*	0.42	0.13	23.5	500	7.8	(<4)	19.7
	70	C_9	50		1.01	0.12	21.8	825	9.1	(<4)	12.7
	70	TMB^2	50		1.10	0.18	28.7	575	13.8	(<4),(~9.8)	14.9
	80	TMB^2	50		1.30	0.24	27.7	845	13.8	(<4),(~9.8)	13.9

[a] Cylindrical pore sizes of entrances calculated from N_2 isotherms "desorption branch" using BJH method. [b] Thickness calculated by subtracting the pore cavity size (R) from the lattice constants. [c] S/P (%) is the percentage of copolymers to TMOS in the composition domains, [amount of copolymer/amount of TMOS × 100]. [d] Additive hydrocarbons (alkanes, and 1,3,5-trimethylbenzene) to the lyotropic phase domains. [e] Cage monoliths synthesized by lyotropic phase systems. [f] TMB^{0,1,2}, the amount ratio of TMB:copolymer is 0.25:2, 0.5:2, and 1:2, respectively.

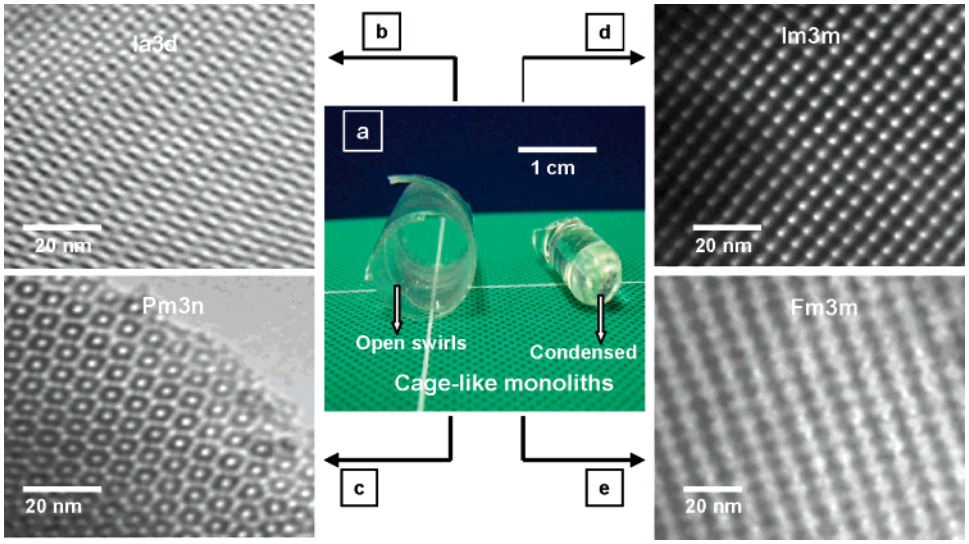

Figure 1. (a) Optically transparent cubic cage-like monoliths HOM-C after (a, left) and before (a, right) removal of the copolymer templates by solvent extraction. TEM micrographs of representative cage monolithic silica structures fabricated in microemulsion systems of the copolymers. Viewed down the (b) [311] and (c) [100] directions of cubic *Ia*3*d* (HOM-C5) and *Pm*3*n* (HOM-C9) fabricated by using F68 template with a TMB:F68 mass ratio of 0.25:2 and of 1:2, respectively. Viewed down the (d) [100] direction of cubic *Im*3*m* (HOM-C1) fabricated by using P123 template with a TMB:P123 ratio of 0.25:2. Viewed down the (e) [110] direction of cubic *Fm*3*m* (HOM-C10) fabricated by using F108 template (F108/TMOS ratio of 80 wt %) with a TMB:F108 mass ratio of 1:2.

were not aged (i.e., without static conditions). The methanol that was initially produced aided the formation of well-homogenized phase as previously reported.[24] The removal of methanol by gentle vacuum at 45−50 °C (Table 1) was necessary to form highly reproducible glassy silica monoliths during the solidification process. Within ~10 min of methanol removal, the resulting viscous liquid changed to an optical gellike material (solid product) and acquired the shape and size of the reaction vessel. To obtain centimeter-sized, crack-free, and shape-controlled silica translucent monoliths (Figure 1a), the resultant translucent silica/copolymer mesophase monoliths were gently dried at room temperature for 3 h and then allowed to stand in a sealed container at 40 °C for 10 h to complete the drying process. The copolymer and the incorporated TMB and alkanes were removed by calcination. The HOM-C solid monoliths were pretreated in N_2 flow of 90 mL min^{-1} for 1 h at 450 °C (heating rate 3 °C min^{-1}). For complete removal of the organic moieties, the monoliths were then treated in O_2 gas for 6 h at 450 °C.

Hydrothermal Treatments of Cage Monoliths. To check the hydrothermal stability of HOM-C, the calcined monolithic samples were first ground into powder. The resultant powder samples (about 250 mg) were then refluxed in deionized water at 100 °C while stirring for different periods of time (from 1 to 30 days). After the refluxing, the samples were filtered and dried at 120 °C.

Analyses. Small-angle powder X-ray diffraction (XRD) patterns for HOM-C materials were measured by using an MXP 18

diffractometer (Mac Science Co. Ltd.) with monochromated Cu Kα radiation with scattering reflections recorded for 2θ angles between 0.3° and 6.5° corresponding to *d* spacings between 29.4 and 1.35 nm. N_2 adsorption−desorption isotherms were measured using a BELSORP36 analyzer (JP. BEL Co. Ltd) at liquid N_2 temperature (77 K) by using the Brunauer−Emmett−Teller (BET) method of surface area and the Barrett−Joyner−Halenda (BJH) analyses of pore size distributions from th e adsorption curve of the isotherms. All samples were pretreated at 300 °C for 8 h under vacuum until the pressure was equilibrated to 10^{-3} Torr. Transmission electron microscopy (TEM) images were obtained by using a JEOL TEM (JEM-2000EXII) operated at 200 kV with a side-mounted CCD camera (Mega View III from Soft Imaging System Co.). The TEM samples were prepared by dispersing the powder particles onto holey carbon film on copper grids. ^{29}Si MAS NMR spectra at room temperature were also measured using a Bruker AMX-500 operated at 125.78 MHz with a 90° pulse length of 4.7 μs. For all samples, the repetition delay was 180 s with a rotor spinning at 4 kHz. The chemical shift scale was externally set to zero for the ^{29}Si signal by using tetramethylsilane.

Results and Discussion

Synthesis of Periodically Cubic Cage Monoliths (HOM-C). Monolithic cage mesostructures with various cubic mesophase geometries can be synthesized over a wide range of composition domains of triblock copolymers ($EO_mPO_nEO_m$) using instant direct-templating strategy in microemulsion systems, as listed in Table 1. This synthesis strategy is simple in terms of fabrication time (minutes) and in composition (copolymers/hydrocarbons/TMOS/H_2O) domains and is efficient in designing ordered cubic cage mesostructures into monoliths that are mechanically stable, optically translucent, macroscopically large scale, and crack-free (Figure 1a). Despite the cage materials being prepared in normal synthesis conditions (see Experimental Section), the monoliths have retained their strength and toughness in terms of transparency for a long time (1 year to date), as previously reported.[24,27,28] Such long-term retention makes these monoliths technologically promising.[1,23] In the instantly preformed microemulsion liquid crystal phases, the addition of TMOS to copolymer/hydrocarbon domains formed well-homogenized sol−gel mixtures, particularly when the copolymer concentration was high (70−90 wt %). An acidified aqueous solution ($1 \leq pH \leq 1.3$) was added to the mixture domains to quickly achieve the desired liquid-crystal phase and then to promote hydrolysis of the TMOS around the liquid-crystal phase assembly of the copolymer surfactants. Under these acidic conditions, viscous gellike copolymer−silica phase structures were successfully fabricated in rapid gelation (~10 min). Despite such rapid gelation, long-range ordered frameworks with cage geometrical structures were attained (Figures 1b−e and 2). The addition of hydrocarbons to the mixture domains can successfully form a quaternary system and can significantly accelerate the polymerization of inorganic species while improving the mesopore periodicity.[24] Furthermore, the instantly preformed liquid-crystal phase templating strategy,[24] in principle, reveals new insight into actual control of mesophase geometry and cage mesopore organization (Table 1), and such control is an extension of the direct templating method.[27] Therefore, cage monoliths with various 3D geometries were feasibly fabricated (Table 1). Here, the TEM images (Figures 1b−e) are direct, real-space evidence that long-range ordered cage pores in large-scale domains along the incidences are characteristic of the monoliths (designated as HOM-C). The most prominent feature of these HOM-C monoliths was uniform arrangement and continuous ordering along all directions without distortion, indicating the integrity of the cubically ordered cage frameworks with *Ia*3*d*, *Pm*3*n*, *Im*3*m*, and *Fm*3*m* symmetries (Figures 1b−e).

Cubic cage-like *Ia*3*d* monoliths (HOM-C5) were successfully fabricated here for the first time in microemulsion systems of F68 ($EO_{80}PO_{27}EO_{80}$) copolymer (Table 1). The XRD pattern (Figure 2Aa) shows finely resolved Bragg diffraction peaks, which are indicative of highly ordered cubic structure. Based on the assignment of the diffraction lines according to this XRD profile (see Supporting Information S1), the cubic structure was assigned to *Ia*3*d* symmetry.[11,24] The representative TEM images oriented along the [311] (Figure 1b) and [111] zone axes (see Supporting Information S2) provide direct evidence that the gyroid minimal surface can describe the cubic *Ia*3*d* morphology of the cage HOM-C5 monoliths.[11] The lattice constant estimated from the TEM image agreed relatively well with those calculated from the XRD pattern ($a = d_{211}\sqrt{6}$). Such agreement is strong evidence that the *Ia*3*d* domains are characteristic of cubic cage structures.

Monoliths with primitive cubic *Pm*3*n* cage structures (HOM-C9) were fabricated based on phase transition induced by the addition of a high amount of TMB to the cubic *Ia*3*d* phase domains of F68 (see Table 1). The XRD pattern reveals three poorly resolved high-intensity reflection peaks (Figure 2Ab) with respective *d* spacing ratios of $\sqrt{4}:\sqrt{5}:\sqrt{6}$, which are indicative of primitive cubic phases with *m*3*m* or *m*3*n* point groups. The low resolution of these diffraction lines indicates that the XRD profile is not adequate to identify primitive cubic symmetry. However, the unique additional weak intensity peaks in the range $1° \leq 2\theta \leq 3°$ were assigned to high-order cubic *Pm*3*n* structures. TEM images recorded along the [100] (Figure 1c) and [210] directions (see Supporting Information S2) show evidence of well-ordered pores connecting to large regions of domains, consistent with the reported SBA-1 of cubic cage structures with *Pm*3*n* space group.[13,19] The interplanar distance of the [100] plane estimated from the TEM image (Figure 1c) agrees well with the d_{210} spacing of cubic *Pm*3*n* diffraction pattern.

The dominant body-centered cubic (bcc) *Im*3*m* cage monoliths (HOM-C1) were synthesized for the first time by using copolymer P123 ($EO_{20}PO_{70}EO_{20}$) at low P123/TMOS composition ratio of 35 wt %. This cubic *Im*3*m* mesophase

(27) (a) Attard, G. S.; Glyde, J. C.; Göltner, C. G. *Nature* **1995**, *378*, 366. (b) Göltner, C. G.; Henke, S.; Weissenberger, M. C.; Antonietti, M. *Angew, Chem. Int. Ed.* **1998**, *37*, 613.

(28) (a) Melosh, N. A.; Lipic, P.; Bates, F. S.; Wudl, F.; Stucky, G. D.; Fredrickson, C. H.; Chmelka, B. F. *Macromolecules* **1999**, *32*, 4332. (b) Yang, H.; Shi, Q.; Tian, B.; Xie, S.; Zhang, F.; Yan, Y.; Tu, B.; Zhao, D. *Chem. Mater.* **2003**, *15*, 536. (c) Melosh, N. A.; Davidson, P.; Feng, P.; Pin, D. J.; Chmelka, B. F. *J. Am. Chem. Soc.* **2000**, *122*, 823. (d) Rozière, J.; Brandhorst, M.; Dutartre, R.; Jacquin, M.; Jones, D. J.; Vitse, P.; Zajac, J. *J. Mater. Chem.* **2001**, *11*, 3264.

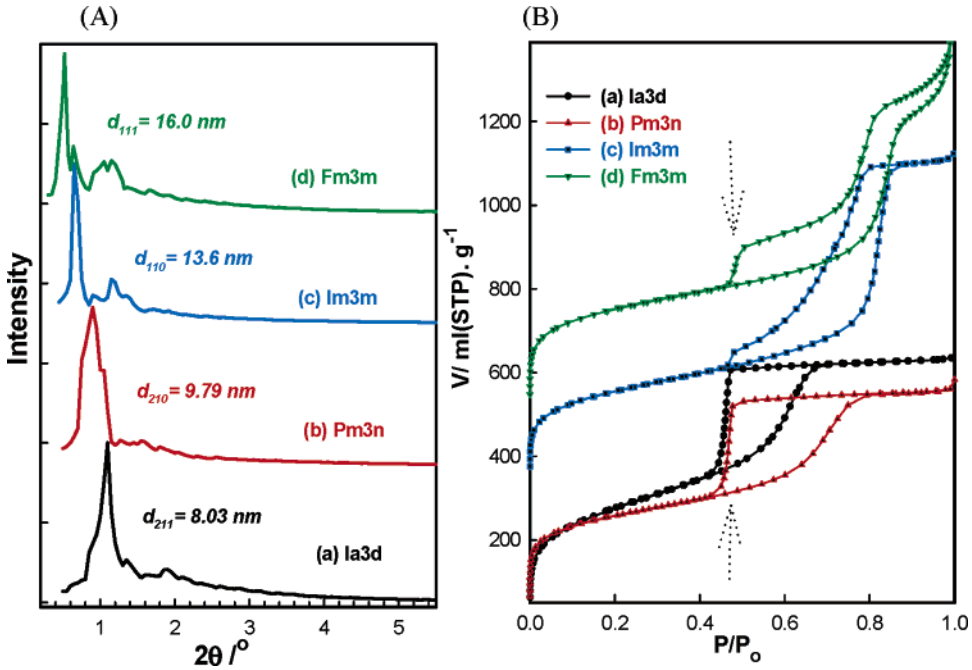

Figure 2. (A) XRD patterns; (B) N_2 adsorption/desorption isotherms of calcined mesoporous silica monoliths with cage-like structures fabricated in microemulsion systems of the block copolymers. (a) Cubic *Ia*3*d* (HOM-C5) and (b) cubic *Pm*3*n* (HOM-C9) fabricated by using F68 template with a TMB:F68 mass ratio of 0.25:2 and of 1:2, respectively. (c) Cubic *Im*3*m* (HOM-C1) and (d) cubic *Fm*3*m* (HOM-C10) fabricated by using F108 template (F108/TMOS ratio of 80 wt %) with a TMB:F108 mass ratio of 0.25:2 and of 1:2, respectively. Isotherms c and d were shifted vertically by 340 and 510 mL STP g^{-1}, respectively.

was abundant, however, when F108 ($EO_{141}PO_{44}EO_{141}$) was used as a template in both the lyotropic and microemulsion systems at a wide range of F108/TMOS mass ratio of 35−80 wt % (Table 1). The XRD pattern for the HOM-C1 (Figure 2Ac) shows well-resolved diffraction lines in the region $0.5 \leq 2\theta \leq 2.4°$, indicating a high degree of cubic *Im*3*m* structural ordering with a large lattice constant up to 20 nm (see Supporting Information S1). The TEM image (Figure 1d) clearly shows an arrangement of white dots with large-scale domains, which is an arrangement identified as regular cage pore arrays. This pattern agrees well with previous TEM micrograph images of SBA-16 structure, which has (bcc) cubic *Im*3*m* symmetry with I-WP minimal surface morphology.[13]

Cubically ordered mesoporous silica cage-like monoliths (HOM-C10) with *Fm*3*m* symmetry were synthesized in microemulsion systems of F108 copolymer over a wide range of phase composition domains (Table 1). The XRD pattern (Figure 2Ad) reveals two intense, sharp reflection planes at $2\theta \leq 0.6°$ respectively assigned to diffraction planes with *d* spacing ratios of $\sqrt{3}$ and $\sqrt{4}$, and reveals well-resolved lower intensity peaks in the region $0.8 \leq 2\theta \leq 2.5°$ respectively assigned to $\sqrt{8}$, $\sqrt{11}$, $\sqrt{12}$, $\sqrt{16}$, $\sqrt{22}$, $\sqrt{32}$, $\sqrt{36}$, and $\sqrt{44}$, which are ratios consistent with cubic *Fm*3*m* structure (single phase) with large lattice constants ranging from 235 to 287 Å.[24] The diffraction lines, namely, the sharp (311) and (222) lines, were evidence of the formation of the spherical cage cubic *Fm*3*m* phase with long-range order domain sizes.[14,22,24] Figure 1e shows a typical TEM image of HOM-C10 monoliths oriented along the [110] direction, in which large domain sizes of remarkably uniform and extensive ordered pore cages were observed. In the interior of these spherical pores (cavities), well-organized 4-fold symmetric grains were clearly connected between the cage network (Figure 1e), suggesting that the cubic *Fm*3*m* cages had uniform pore cavities, even when the pore cavities were large, about 14 nm in diameter (Table 1). Such pore geometries are expected to be favorable for facilitating the efficacious accessibility of large molecules.[14]

Further evidence of the shape- and size-controlled cage mesostructured monoliths is the N_2 isotherms (Figure 2B). The large type-H_2 hysteresis loops and well-defined steepness of the isotherms indicate large, uniform cage structures.[22] Both the isothermal shape and P/P_o (0.45−0.5 range) of the capillary evaporation are similar for all HOM-C monoliths, indicating that the sizes of the entrance pores were less than 4.0 nm (as indicated by arrows in Figure 2B), despite the increase in sizes of spherical interior cavities (Table 1 and Supporting Information S3). With HOM-C cages, enlarged open-entrance pores (trimodal or bimodal) were evident (Figure 2Bc,d); however, the shift toward higher P/P_o for the desorption isotherms indicates other enlarged pore entrances up to 9.8 nm in size were connected, without loss of cage periodicity.[22] For all HOM-C cage structures, one of these entrance sizes was narrower, <4 nm (see Supporting Information S3), independent of the various synthesis phase conditions or templated copolymers that have various molecular natures (Table 1). The other dominant entrance sizes gradually increased with increasing copolymer/TMOS ratio and increasing solubilization of hydrocarbon in the phase composition domains (Table 1). This finding indicates significant control over the size and shape of entrance pores (see Scheme 1). Our results indicate that the generation of the enlarged open-entrance pore systems here was due to the expansion of the copolymer micelles. This swelling action, in addition to causing an increase in the size of both connecting pores and spherical interior cavities, induced a conformation change in the surface curvature of micelle to

Scheme 1. Simple Model of the Possible Distribution of the Open-Entrance Pore Sizes Connecting One Cavity of the Cage-like Pore Nanostructured Monoliths[a]

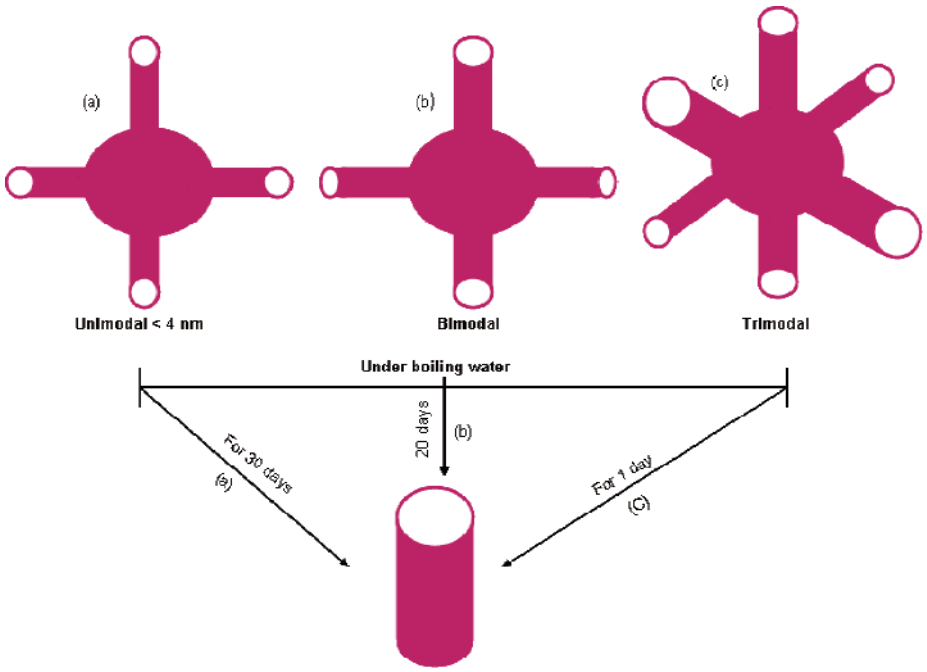

[a] The time dependence of the formation of cylindrical pore under extreme hydrothermal treatments indicated the effect of shape-selective structures on the stability of the cage character.

a curvature that is more compatible with the preferred mesophase structure formed according to the surfactant geometry. This finding provides strong evidence that the pore-entrance enlargement and the phase geometrical change were the main causes of the generation of the HOM-C cage systems that have enlarged open-entrance pores (Table 1).

The microporosity of the HOM-C monoliths ranged from 0.05 to 0.24 cm^3/g, similar to the ranges reported for FDU-1 synthesized under higher temperature and longer reaction time.[22a,b] The existence of the HOM-C micropores was strongly affected by the unit numbers of EO_m blocks of the copolymer templates and by the solubilization of hydrocarbons into the phase domains, as outlined in Table 1. In general, the instant direct-templating strategy provides appreciable textural parameters of specific surface area (1000 m^2/g), mesopore/micropore volume, thick-walled frameworks up to 20 nm thick, and enlarged entrances and cavity sizes with significant retention of cage nature and uniformity of mesostructures (Table 1).

Several key factors affect the formation of the large mesoscopically ordered cage structures (HOM-C) in the final products of templated copolymers ($EO_mPO_nEO_m$). The first factor is that the formation of the true transparent liquid-crystal phase in both lyotropic and microemulsion systems (one single phase even at high copolymer concentration of 90 wt %) was sufficient to retain the anisotropic organization of the crystalline cage phases even after interaction between the silica species and the EO blocks of template to form rigid condensed framework matrixes, as clearly revealed by the TEM and XRD profiles (Figures 1 and 2A). Another factor is that the copolymer molecular weight and the block composition EO/PO ratios crucially influence the phase geometries of the amphiphile.[29] High composition ratios of EO/PO block copolymers, in general, were likely to form ordered cage geometries in wide phase composition domains.[13] For example, the dominated cage structures (cubic *Im*3*m* and *Fm*3*m* phases) were formed with the F108 system at large phase domains compared with the HOM-C cages of P123 and F68 systems (Table 1), indicating the significant role of the copolymer structures in determining the ordered cage mesostructures. The fabrication of these oriented nanostructured materials demonstrated actual control over the mesophase shape, domain, and morphology.[24] Another factor is that, in microemulsion systems, the addition of hydrocarbons to the phase aggregates not only caused enlargement of the cavities and entrance-pore sizes and changes in the surfaces with high interfacial curvature of micelles but also induced cross-linking of inorganic silica oligomers to form dense, ordered cage frameworks in large-scale domains. The type of copolymer/hydrocarbon interaction and the degree of hydrocarbon solubilization might be used to control the substantial swelling and the changes in geometrical phases during the synthesis of HOM-C cage monoliths.[24] TMB was an effective solubilizing agent by its increased ability to penetrate the PO blocks and to enlarge the pore sizes compared with straight alkyl chain hydrocarbons as a solubilizing agent. Finally, another factor is that, in the lyotropic (cosolvent-free) phase domains, the change in copolymer concentration led to the following significant features (Table 1): (i) increase in the micellar size and volume fraction caused an increase in interlayer *d* spacing and cavity pore sizes of the mesophase composition that had

(29) (a) Holmqvist, P.; Alexandridis, P.; Lindman, B. *J. Phys. Chem. B* **1998**, *102*, 1149. (b) Wanka, G.; Hoffmann, H.; Ulbricht, W. *Macromolecules* **1994**, *27*, 4145. (c) Yang, L.; Alexandridis, P.; Steytler, D. C.; Kositza, M. J.; Holzwarth, J. F. *Langmuir* **2000**, *16*, 8555.

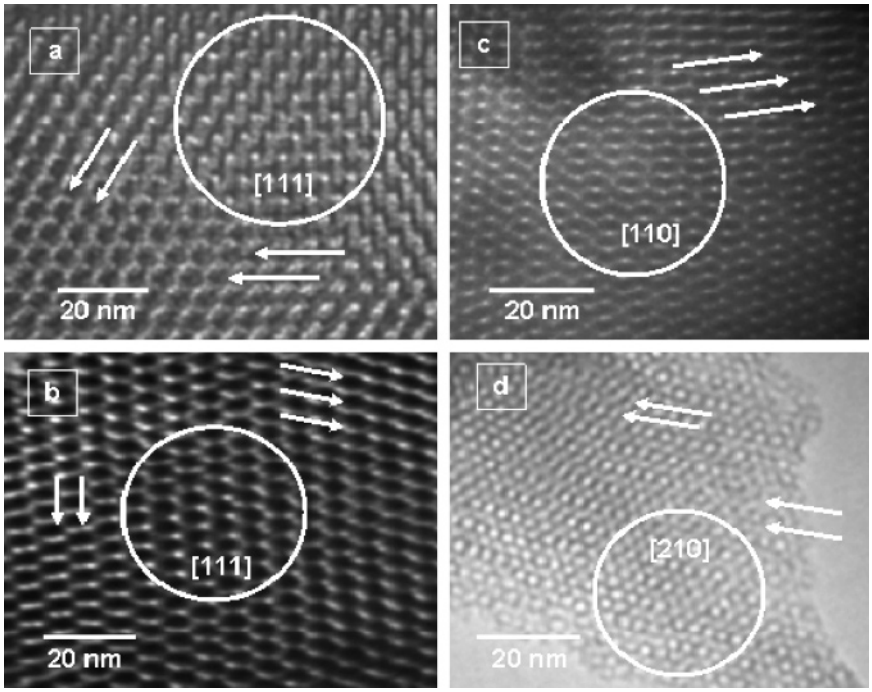

Figure 3. TEM micrographs of representative cage monolithic mesopore structures after hydrothermal treatment in boiling water for 1 day of (a) cubic *Fm*3*m* (HOM-C10), (b) cubic *Im*3*m* (HOM-C1), (c) cubic *Ia*3*d* (HOM-C5), and (d) cubic *Pm*3*n* (HOM-C9). Arrows indicate the distortion "defects" in this pore ordering caused by the hydrothermal treatments. Circles indicate the retention of ordered pore cages.

higher copolymer concentration, (ii) the micellar aggregate-assembly at each phase composition might have acted as a driving force for the preferred shape formation based on the molecular geometry of the phase structures, and (iii) the pore sizes increased as a function of the core (PO) and corona (EO) block lengths, whereas the pore size was strongly affected by the hydrophobic block (PO) length.[24c] This effect of EO-block on the cage pore sizes of HOM-C monoliths differs from that for materials synthesized by using EO_m-BO_nEO_m copolymers,[30a] where the pore size of these materials decreases with large EO-blocks of template, but is similar to that for nanocasted silica mesophases fabricated by using alkyl-oligo(ethylene oxide) (C_xEO_y) surfactants as templates.[30b]

Hydrothermal Stability of Cage Silica Monoliths (HOM-C). The thick-walled pores and high degree of siloxane unit cross-linking in the frameworks of the monoliths fabricated here using the instant direct-templating synthesis strategy without requiring any aging time or high temperature are particularly important for practical applications of HOM-C cage structures. ^{29}Si NMR spectra (see Supporting Information S4) revealed higher Q_4/Q_3 ratios of ≥ 6 (where $Q_n = Si(-OSi-)_n(OH)_{4-n}$) for all calcined or even solvent-extracted HOM cage mesostructures. These higher ratios are indicative of fully cross-linked HOM-C cage framework matrixes,[3,25,26] and consequently, much more rigid siloxane linkages that would have to stabilize the architecture wall to withstand hydrothermal treatment for a month (or even longer) without loss of the mesoporosity structures, despite the locally disordered atomic scale of these HOM-C cage frameworks. More important for practical application is the significant retention of ordering cages of hydrotreated samples achieved even after a long time period of treatment (1−3 days). TEM micrographs (Figure 3) show the first clear evidence that well-ordered pores that are connected over sufficiently large-scale domains were retained for all cage structures, despite the hydrothermal treatment under refluxing in boiling water. However, the TEM images also reveal defects (indicated by arrows in Figure 3), suggesting distortion in the cage pores during hydrothermal treatment.

XRD patterns (Figure 4) show further evidence that the hierarchical mesopore cage frameworks were retained for a month. However, the diffraction patterns (Figures 4b−d) show well-resolved high order reflection peaks, indicating significant hydrothermal stability of cubic *Fm*3*m* cage monoliths. For longer boiling times (>10 days), although the intensity and resolution of the diffraction peaks were less pronounced, the peaks still indicate the retention of HOM-C cage frameworks. In general, these results indicate that degradation of the pore-wall architecture occurred after a long treatment time (>10 days) in boiling water; however, this degradation did not ultimately lead to loss or collapse of the cage mesostructured geometry, as evidenced by the slight changes in d_{-111} value or lattice constants ($a = d_{111}\sqrt{3}$) of the cubic *Fm*3*m* cage structure (Figure 4).

The N_2 isotherms of the hydrotreated HOM-C cage monoliths (Figure 5) clearly revealed the most informative evidence of the extent of the distortion and loss of uniformity of the entrance pores.[26b] The shape of the isotherms of the cage structures with (Figure 5B) and without (Figure 5B) enlarged open-entrance pores remained virtually unchanged after boiling for 1 day, indicating the retention of the cage geometries. For longer boiling times (>3 days), the adsorption−desorption branches shifted to higher P/P_o, while the desorption branch at the lower limit of hysteresis was still pronounced even after boiling for 10 days. This shift indicates

(30) (a) Yu, C.; Fan, J.; Tian, B.; Stucky, G. D.; Zhao, D. *J. Phys. Chem. B* **2003**, *107*, 13368. (b) Smarsly, B.; Polarz, S.; Antonietti, M. *J. Phys. Chem. B* **2001**, *105*, 10473.

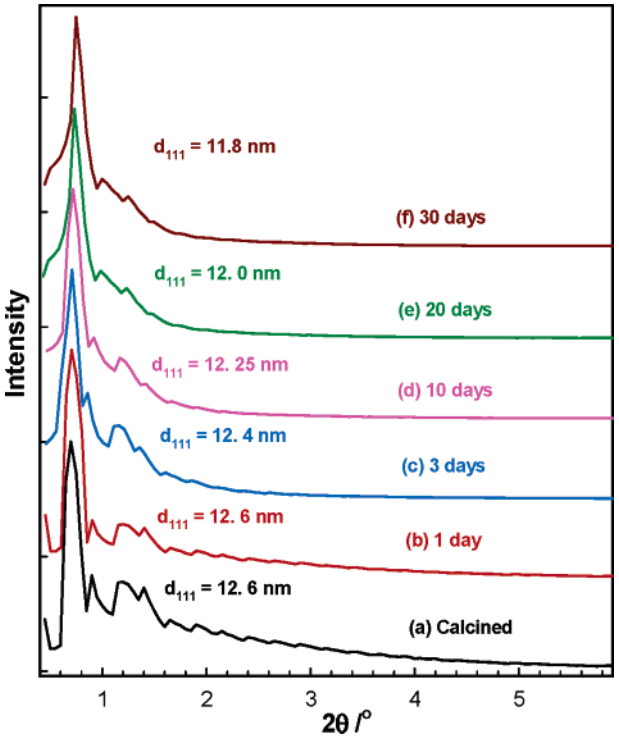

Figure 4. XRD patterns of calcined cubic *Fm*3*m* cage monoliths (HOM-C10) synthesized in a microemulsion system of F108 copolymer by addition of C_9-alkane (nonane) to the phase domains at F108/TMOS of 70 wt %. (a) Before and (b−f) after hydrothermal treatments in boiling water from 1 to 30 days.

the development of other connecting pores (Figure 5A) or larger sizes of entrance pores (Figure 5B). However, for longer boiling times (>10 days), the hysteresis loop changed from H_2- to H_1-type, indicating that the desired and stable shape of the cage with connecting pore systems might be cylindrical in nature (see Scheme 1).[22] Both sets of isotherms (Figures 5A and 5B) indicate loss in the cage character of HOM-C mesostructures at longer boiling times (>20 days), while desired structural geometry was attained, as evidenced from the XRD patterns (Figure 4). Based on the N_2 isotherms (Figure 5), the size and shape of connecting pores and the nature of the spherical cavity of the cage geometry crucially influenced the retention of the HOM-C cage character under long-term hydrothermal treatment in boiling water (Scheme 1), as evidenced by the stability of the cage nature previously reported for 2D hexagonal (PSU-1) and cubic *Fm*3*m* (FDU-1) materials during hydrothermal studies.[26b,c]

The broader line width of pore size distribution curves (data not shown) and the shift to larger pore sizes and lower specific surface area (insert in Figure 5) indicate the extent of degradation of the HOM-C cage pore frameworks. In addition, hydrothermal treatment also apparently caused thinner walled pores; however, the increase in the hydrothermal treatment time caused hydrolysis of the siloxane (Si−O−Si) bridges in the framework pores.[25,26] These results are clear evidence of the significant dissolution of the pore wall architectures during the refluxing in boiling water, particularly for long-time treatment (>10 days). On the other hand, the remarkable hydrothermal stability of these HOM-C monoliths (Figures 3−5) indicated that the fabricated cage structures, in particular, had thick-walled pores and a high degree of cross-linking framework, as evidenced from the retention cage character under long-term refluxing. However, during the HOM-C fabrication design, the silica condensation conditions were adequate to improve the interaction between silica and copolymer species and to fabricate highly ordered silica monoliths (HOM-C) that have thick-walled network matrixes. In general, our synthetic strategy, namely, an instant direct-templating method, shows promise in fabricating highly hydrothermally stable cage frameworks, in which no special synthesis treatment is required to stabilize this framework.[25,26]

Conclusion

Our design strategy provides a general and efficient route to control the shape and size of liquid-crystalline phase geometries and control the extended long-range ordering in

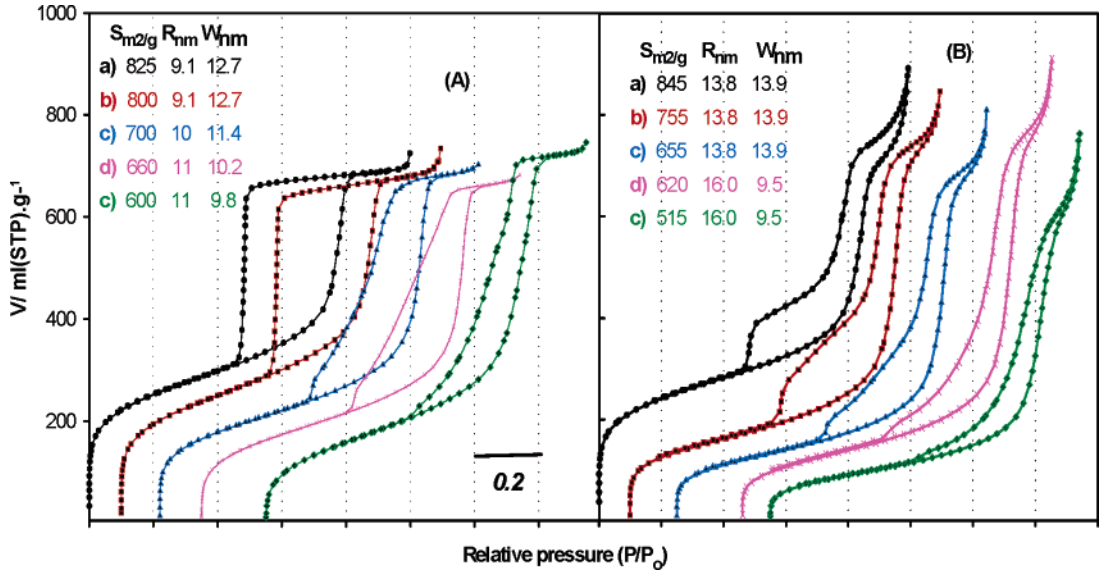

Figure 5. (A) and (B) Representative of N_2 isotherms of different cage structural shapes under hydrothermal treatments in boiling water for (b) 1, (c) 3, (d) 10, and (e) 20 days, respectively. (A-a) Calcined cubic *Fm*3*m* (HOM-C10) monoliths (fabricated as shown in Figure 4a**)** and (B-a) calcined cubic *Fm*3*m* (HOM-C10) monoliths (fabricated as shown in Figure 2d**)**. Insets are the corresponding textural parameters of *S*, BET surface area, *R*, interior pore cavity, and *W*, wall thickness of the samples before and after the hydrothermal treatments.

the final cage mesostructured replicas. With this strategy, a variety of mesoscopically ordered cage structures can be easily fabricated with promising possibilities in controlling the pore dimensions over a wide range (5−15 nm) in both lyotropic and microemulsion systems of copolymers. Well-resolved unique reflection in the XRD patterns and crystal orientation in TEM profiles from this current study revealed the highly ordered structures, indicating reliable identification of cubic structural geometries. The ability to form cage mesostructured monoliths that are macroscopically large-scale glass (crack-free), have mesoscopically ordered domains, tunable interior cavities with uniform pore entrances, and hydrothermally stable frameworks, could make these monoliths an attractive design for promising applications.[1]

Supporting Information Available: Additional details and figures (PDF). This material is available free of charge via the Internet at http://pubs.acs.org.

CM050013H